Letters

International Journal of Bifurcation and Chaos, Vol. 20, No. 1 (2010) 135–144

DOI: 10.1142/S0218127410025454

GENERATING 3-SCROLL ATTRACTORS FROM ONE CHUA CIRCUIT

ZERAOULIA ELHADJ
Department of Mathematics,
University of Tébessa, 12002, Algeria
zeraoulia@mail.univ-tebessa.dz
zelhadj12@yahoo.fr

J. C. SPROTT
Department of Physics, University of Wisconsin,
Madison, WI 53706, USA
sprott@physics.wisc.edu

Received February 26, 2008; Revised May 21, 2009

This paper reports the finding of a 3-scroll chaotic attractor with only three equilibria obtained via direct modification of Chua's circuit. In addition, it is shown numerically that the new system can also generate one-scroll and two-scroll chaotic attractors.

Keywords: Modified Chua's equation; 3-scroll chaotic attractor; two-variable characteristic piecewise linear function.

1. Introduction

Chaos is the idea that a system will produce very different long-term behaviors when the initial conditions are perturbed only slightly. Piecewise linear chaotic systems, for example [Altman, 1993; Chua *et al.*, 1986; Aziz-Alaoui, 1999; Sprott, 2000; Zeraoulia, 2006, 2007], are used to construct simple electronic circuits with applications in electronic engineering, especially in secure communications [Kal'yanov, 2003; Karadzinov *et al.*, 1996; Mahla & Palhares, 1993]. Circuits also provide a very useful vehicle for studying chaos as well as easy applications. Chua's circuit [Chua *et al.*, 1986] is one of the most interesting examples of chaos in circuit theory. This circuit consists of an inductor, two capacitors, and a nonlinear resistor, all in parallel, and a controlled resistor in series between the two capacitors as shown in Fig. 1. This circuit is structurally the simplest and dynamically the most complex member of Chua's circuit family [Chua *et al.*, 1986]. Chua's circuit is given by the following closed-form dimensionless equations:

$$\begin{cases} x' = \alpha(y - f(x)), \\ y' = x - y + z, \\ z' = -\beta y, \end{cases} \tag{1}$$

where α and β are constant parameters and

$$f(x) = m_1 x + \frac{1}{2}(m_0 - m_1)(|x+1| - |x-1|) \tag{2}$$

is the characteristic function of system (1)–(2), with m_0, m_1 the slopes of the outer and the inner regions. System (1)–(2) gives a chaotic attractor called the *double-scroll attractor* [Chua *et al.*, 1986]. The original piecewise-linear characteristic of Chua's equation has been generalized by many researchers using various different forms for the nonlinearity. For example, the original piecewise-linear function can

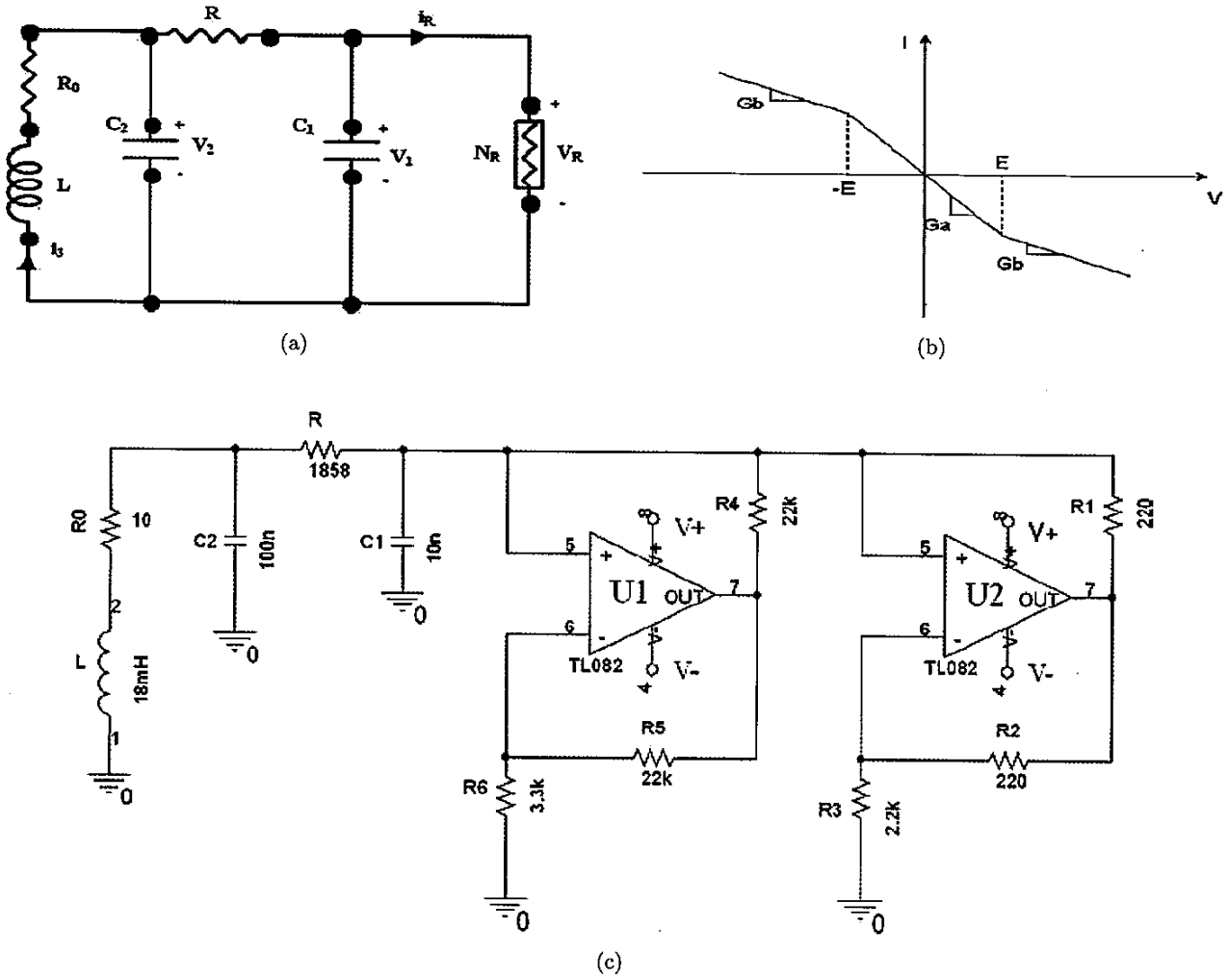

Fig. 1. (a) A circuit diagram for Chua's oscillator. (b) Typical i–v characteristics of Chua's diode. (c) Circuit realization scheme [Billota *et al.*, 2007a].

be replaced by a discontinuous function [Khibnik *et al.*, 1993; Lamarque *et al.*, 1999], a C^∞ "*sigmoid function*" [Mahla & Palhares, 1993], a cubic polynomial $c_0x^3+c_1x$ [Altman, 1993; Hartley & Mossaybei, 1993; Khibnik *et al.*, 1993], or an "*abs*" nonlinearity $x|x|$ [Tang *et al.*, 2003].

In fact, the piecewise-linear (PWL) continuous chaotic systems can also generate various attractors, even the more complex multiscroll attractors. For PWL continuous systems and multiscroll attractors, there are many works including the generation and circuit design for multiscroll chaotic attractors [Lü *et al.*, 2004, 2006]. Indeed, a family of n-scroll chaotic attractors was introduced by Suykens and Vandewalle in [1993]. Chaotic attractors with multiple-merged basins of attraction were studied by Lü *et al.* in [2003] using a switching manifold approach. In [Yalcin *et al.*, 2002] a family of scroll grid attractors was presented using a step function approach including one-dimensional (1-D) n-scroll, two-dimensional (2-D) $(n \times m)$-grid scroll, and three-dimensional (3-D) $(n \times m \times l)$-grid scroll chaotic attractors. In [Lü *et al.*, 2004a, 2004b, 2006], Lü *et al.* proposed with rigorous theoretical proofs and experimental verification the hysteresis series and saturated series methods for generating 1-D n-scroll, 2-D $(n\times m)$-grid scroll, and 3-D $(n\times m\times l)$-grid scroll chaotic attractors. In [Yu *et al.*, 2008, 2009], Yu *et al.* generated $2n$-wing and $n \times m$-wing Lorenz-like attractors from a Lorenz-like system and a modified Shimizu–Morioka model, respectively. Finally, using a thresholding approach, Lü *et al.* generated multiscroll chaotic attractors [Lü *et al.*, 2008].

One of the basic properties of multiscroll attractors is that they surround a large number of equilibrium points. In this paper, we report the finding of a *three-scroll chaotic attractor* but with only three equilibria rather than more as in the usual case where this attractor requires at least five equilibria [Aziz-Alaoui, 1999, and references therein]. In addition, it is shown numerically that the new system (3)–(4) below can generate the classical one-scroll and two-scroll chaotic attractors.

This paper is organized as follows. In the following section, we discuss the model, and then we give several basic properties including equilibrium points and their stability in order to characterize the three-scroll chaotic attractor. Some numerical simulations confirming the theory are given and discussed in Sec. 3. The final section gives some conclusions.

2. The Proposed Model

In this paper, a new piecewise-linear version of Chua's circuit (1)–(2) is proposed where we replace the characteristic function (2) by a piecewise-linear function (in the x, z variables) given by:

$$h_a(x,z) = \begin{cases} f(x), & |z| \geq a, \\ -f(x), & |z| \leq a, \end{cases} \tag{3}$$

where a is a positive parameter. The proposed function has the advantage that it has two variables x and z and it has not been previously proposed or studied. Note that $h_a(x,z)$ is an odd-symmetric discontinuous function (except for $a = 0$ or $a = m_1 - m_0/m_1$). A 3-D graph of Eq. (3) is shown in Fig. 2. Hence, the new system is given by:

$$\begin{cases} x' = \alpha(y - h_a(x,z)) \\ y' = x - y + z \\ z' = -\beta y. \end{cases} \tag{4}$$

Suppose that $m_0 < 0$ and $m_1 > 0$. Then one has a new continuous-time, three-dimensional, autonomous, piecewise-linear system. We have discovered that the new model (3)–(4) generates various chaotic attractors including the classical 1-scroll, double-scroll, and three-scroll chaotic attractors. The equation (3)–(4) is piecewise-linear, which simplifies its circuitry realization. This fact is very important because many works have been devoted to building simple electronic chaotic circuits with piecewise-linear functions [Chua & Lin, 1990; Altman, 1993; Hartley & Mossaybei, 1993; Karadzinov *et al.*, 1996; Aziz-Alaoui, 1999; Sprott, 2000]. This situation is quite interesting both theoretically and practically in terms of new chaos generation techniques and possible engineering applications of chaos.

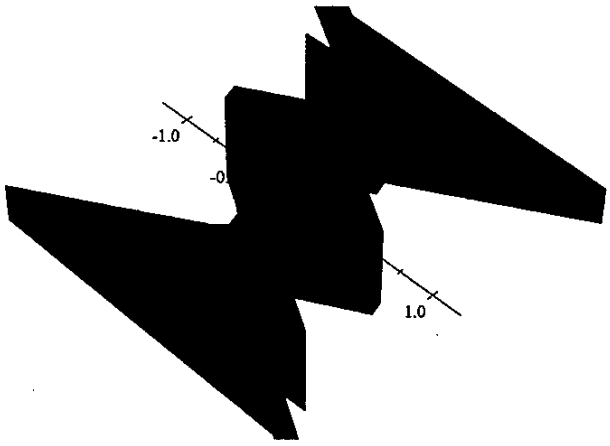

Fig. 2. A 3-D graph of Eq. (3) for $m_0 = -0.43, m_1 = 0.41$ and $a = 1.0$.

We remark that $\lim_{a \to 0} h_a(x,z) = f(x)$, and so it is possible to conclude that the dynamics of system (3)–(4) is very close to the original Chua's circuit (1)–(2) when the bifurcation parameter a is close to zero. This result is confirmed numerically in Sec. 3. For $a < 0$, one has $h_a(x,z) = f(x)$, and so systems (1)–(2) and (3)–(4) are identical. Notably, the system (3)–(4) is not diffeomorphic with the Chua's system (1)–(2) (the two systems are not topologically equivalent) since the system (3)–(4) has nine linear regions with respect to x and z, but the latter has only three regions with respect to the x variable. Dynamically, it is clear that the two systems do not have the same sequence of bifurcations as will be shown in Sec. 3.

The new chaotic system (3)–(4) has several important properties in common with Chua's attractor, but there are some differences between them. It has a natural symmetry under the coordinate transformation $(x,y,z) \to (-x,-y,-z)$, which persists for all values of the system parameters. The divergence of the flow for system (3)–(4) is given by:

$$\nabla V = \frac{\partial x'}{\partial x} + \frac{\partial y'}{\partial y} + \frac{\partial z'}{\partial z} = \begin{cases} -\alpha m - 1, & |z| \geq a \\ \alpha m - 1, & |z| \leq a, \end{cases} \tag{5}$$

where

$$m = \begin{cases} m_1, & |x| \geq 1 \\ m_0, & |x| \leq 1 \end{cases}.$$

Thus if $\alpha > \max(1/m_0, -(1/m_1))$, then the system (3)–(4) has a bounded, globally attracting ω-limit set, and it is dissipative just like Chua's system (1)–(2). The variation of the volume $V(t)$ of a small element $\delta\Omega(t) = \delta x \delta y \delta z$ is determined by the divergence given in Eq. (5), and in this case the exponential contraction rate is

$$\delta\Omega(t) = \begin{cases} \exp(-\alpha m - 1), & |z| \geq a \\ \exp(\alpha m - 1), & |z| \leq a \end{cases}.$$

Hence, a volume element V_0 is contracted in time t by the flow into a volume element $V_0 \exp((\nabla V)t)$. Then each volume containing the system trajectory shrinks to zero as $t \to +\infty$. Thus, all system orbits will be confined to a specific subset having zero volume, and the asymptotic motion converges onto an attractor. This result has been confirmed by numerical simulations in Sec. 3.

2.1. *Equilibrium points and their stability*

In this section, we suppose that $\alpha > 0$ and $\beta > 0$. Due to the shape of the vector field of system (3)–(4), the phase space can be divided into two principal linear regions denoted by R_1 and R_2:

$$R_1 = \{(x, y, z) \in \mathbb{R}^3 : |z| \leq a\} \tag{6}$$

$$R_2 = \{(x, y, z) \in \mathbb{R}^3 : |z| \geq a\}, \tag{7}$$

in which R_1 is itself divided into three linear regions:

$$\begin{cases} \Omega_1 = \{(x, y, z) \in \mathbb{R}^3 : x \geq 1, |z| \leq a\} \\ \Omega_2 = \{(x, y, z) \in \mathbb{R}^3 : |x| \leq 1, |z| \leq a\} \\ \Omega_3 = \{(x, y, z) \in \mathbb{R}^3 : x \leq -1, |z| \leq a\}, \end{cases} \tag{8}$$

and R_2 is divided into six linear regions:

$$\begin{cases} \Omega_4 = \{(x, y, z) \in \mathbb{R}^3 : x \geq 1, z \geq a\} \\ \Omega_5 = \{(x, y, z) \in \mathbb{R}^3 : |x| \leq 1, z \geq a\} \\ \Omega_6 = \{(x, y, z) \in \mathbb{R}^3 : x \leq -1, z \geq a\} \\ \Omega_7 = \{(x, y, z) \in \mathbb{R}^3 : x \geq 1, z \leq -a\} \\ \Omega_8 = \{(x, y, z) \in \mathbb{R}^3 : |x| \leq 1, z \leq -a\} \\ \Omega_9 = \{(x, y, z) \in \mathbb{R}^3 : x \leq -1, z \leq -a\}. \end{cases} \tag{9}$$

Thus, the system (3)–(4) has nine piecewise-linear regions with respect to the variables x and z, which confirm that this system is topologically different from the original Chua's circuit as mentioned above. In this case, all equilibrium points of system (3)–(4) are given by $X_{\mathrm{eq}(x)} = (x, 0, -x)$ where x is the solution of the equation $h_a(x, -x) = 0$. Thus, one has the following two cases: First, if $a \leq 1 - (m_0/m_1)$, then there exist three equilibrium points for the system (3)–(4) as follows:

$$P^{\pm} = \left(\pm\left(\frac{m_0 - m_1}{m_1}\right), 0, \mp\left(\frac{m_0 - m_1}{m_1}\right)\right) \tag{10}$$

and

$$P^0 = (0, 0, 0),$$

such that $P^+ \in \Omega_6$, $P^- \in \Omega_7$, and $P^0 \in \Omega_2$ as shown in Fig. 3, and the Jacobian matrix evaluated at these equilibria is given as follows:

For $P^{\pm}$ one has:

$$J^{\pm} = \begin{pmatrix} -\alpha m_1 & \alpha & 0 \\ 1 & -1 & 1 \\ 0 & -\beta & 0 \end{pmatrix}, \tag{11}$$

and for P^0 one has:

$$J^0 = \begin{pmatrix} -\alpha m_0 & \alpha & 0 \\ 1 & -1 & 1 \\ 0 & -\beta & 0 \end{pmatrix}. \tag{12}$$

Second, if $a > 1 - (m_0/m_1)$, then only $P^0 \in \Omega_2$ exists (so no equilibrium is in R_1).

The Jacobian matrix evaluated at P^0, is given by

$$J^0 = \begin{pmatrix} \alpha m_0 & \alpha & 0 \\ 1 & -1 & 1 \\ 0 & -\beta & 0 \end{pmatrix}. \tag{13}$$

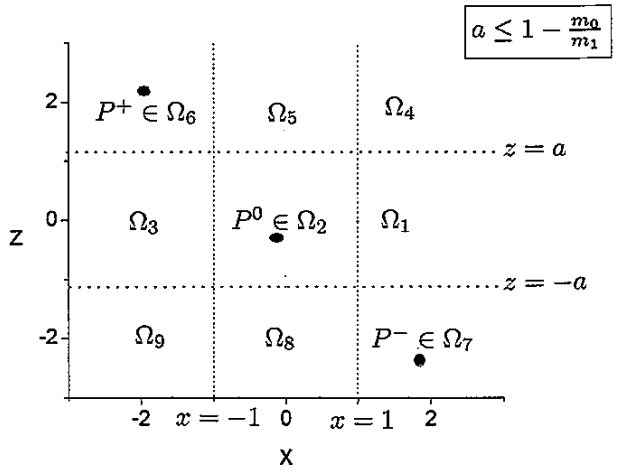

Fig. 3. Equilibria of system (3)–(4).

The eigenvalues are the solutions of the following characteristic cubic equation:

$$P(\lambda) = \lambda^3 + A\lambda^2 + B\lambda + C = 0, \tag{14}$$

where the values of A, B, and C are determined for each equilibrium point as follows:

For $P^{\pm}$ one has in the first case that:

$$\begin{cases} A_1 = \alpha m_1 + 1 \\ B_1 = \beta + \alpha(m_1 - 1) \\ C_1 = \alpha\beta m_1. \end{cases} \tag{15}$$

For P^0 one has in the first case

$$\begin{cases} A_0 = \alpha m_0 + 1 \\ B_0 = -\alpha + \beta + \alpha m_0 \\ C_0 = \alpha\beta m_0, \end{cases} \tag{16}$$

and in the second case one has

$$\begin{cases} A_0 = -\alpha m_0 + 1 \\ B_0 = \beta + \alpha(-m_0 - 1) \\ C_0 = -\alpha\beta m_0. \end{cases} \tag{17}$$

It is easy to show that in the first case one has:

$$C_0 C_1 < 0. \tag{18}$$

Then P^0 and $P^{\pm}$ have different topological types: $P^{\pm}$ is always unstable since C_1 is negative, and therefore one eigenvalue of the Jacobian matrix $J^{\pm}$ is real and positive. Also, note that the two equilibrium points $P^{\pm}$ have the same Jacobian matrix, and thus the two equilibria have the same type of stability in the first case. The exact value of the eigenvalues is obtained by using the Cardan method for solving a cubic equation. On the other hand, the Routh–Hurwitz conditions lead to the conclusion that the real parts of the roots λ (solution of (14)) are negative if and only if $A > 0$, $C > 0$, and $AB - C > 0$. Thus in the first case, $P^{\pm}$ are stable if and only if:

$$\beta > (1 - m_1)\alpha(1 + m_1\alpha) \tag{19}$$

since we assume that $m_1 > 0, \alpha > 0$, and $\beta > 0$, and in the second case P^0 is stable if and only if:

$$\beta > \alpha(1 + m_0)(1 - \alpha m_0). \tag{20}$$

3. Numerical Simulations

In this section, the dynamical behaviors of the system (3)–(4) are investigated numerically where we use an appropriate Poincaré section (value of x at $y = 0$) where the resulting points $\{y_n\}_{n\in\mathbb{N}}$ are computed using the Hénon method [Parker & Chua, 1989], and a set of one of them is recorded after transients have decayed and plotted versus the desired parameter. The calculations of limit sets of the system (3)–(4) were performed using a fourth-order Runge–Kutta algorithm [Parker & Chua, 1989]. Then to determine the long-time behavior and chaotic regions, we numerically computed the largest Lyapunov exponent [Parker & Chua, 1989].

Chaotic behavior implies sensitive dependence on initial conditions with at least one positive Lyapunov exponent. While many algorithms for calculating the Lyapunov exponents would give spurious results for piecewise-linear discontinuous systems, the algorithm used here and given in [Sprott, 2003] works for such cases since the

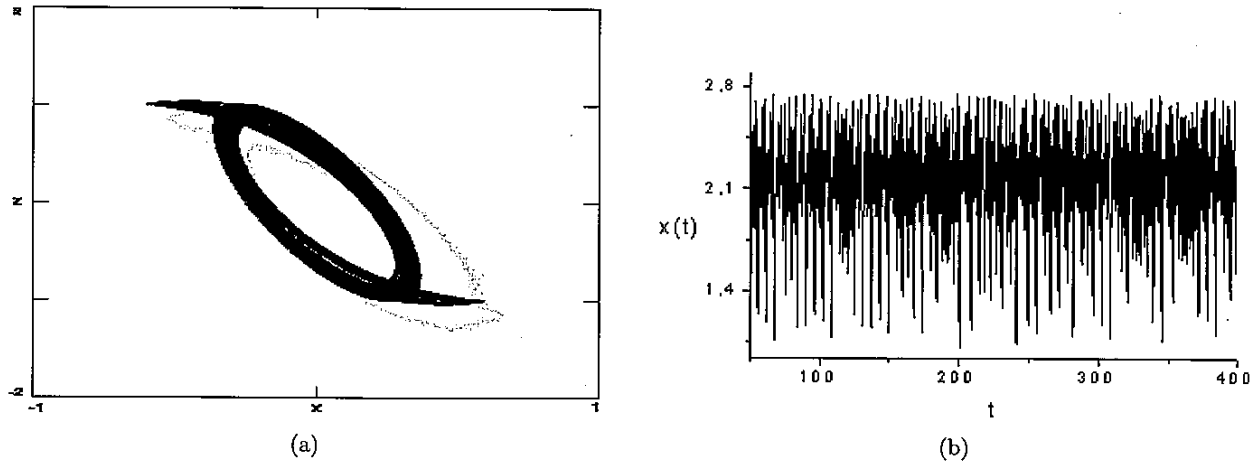

(a) (b)

Fig. 4. (a) Projection onto the x–z plane of a 1-scroll chaotic attractor for $\alpha = 7.0, \beta = 14.0, a = 1.0$. (b) Time waveform of the time series $x(t)$.

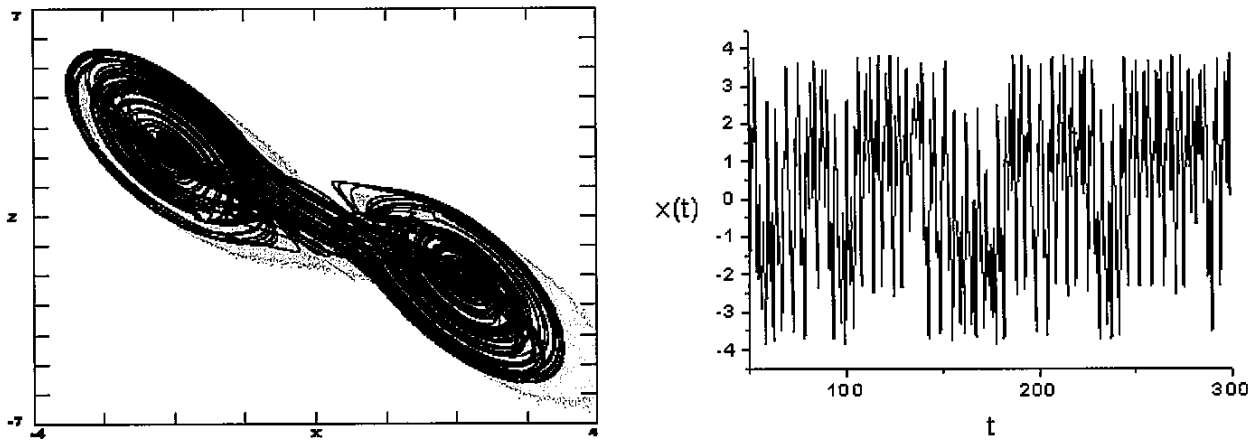

(a) (b)

Fig. 5. (a) Projection onto the x–z plane of a double-scroll chaotic attractor for $\alpha = 10.0, \beta = 14.0, a = 0.1$. (b) Time waveform of the time series $x(t)$.

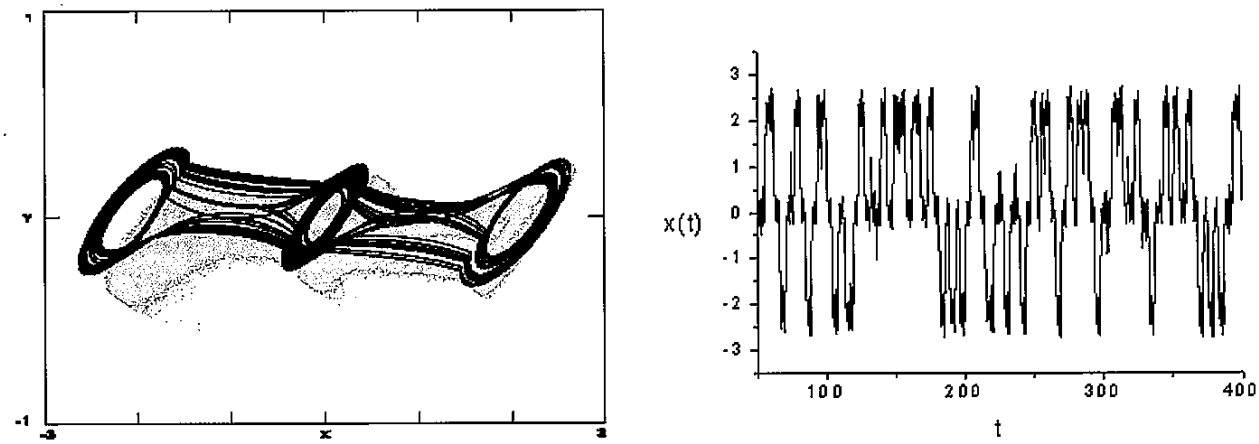

(a) (b)

Fig. 6. (a) Projection onto the x–y plane of a 3-scroll chaotic attractor for $\alpha = 10.0, \beta = 14.0, a = 1$. (b) Time waveform of the time series $x(t)$.

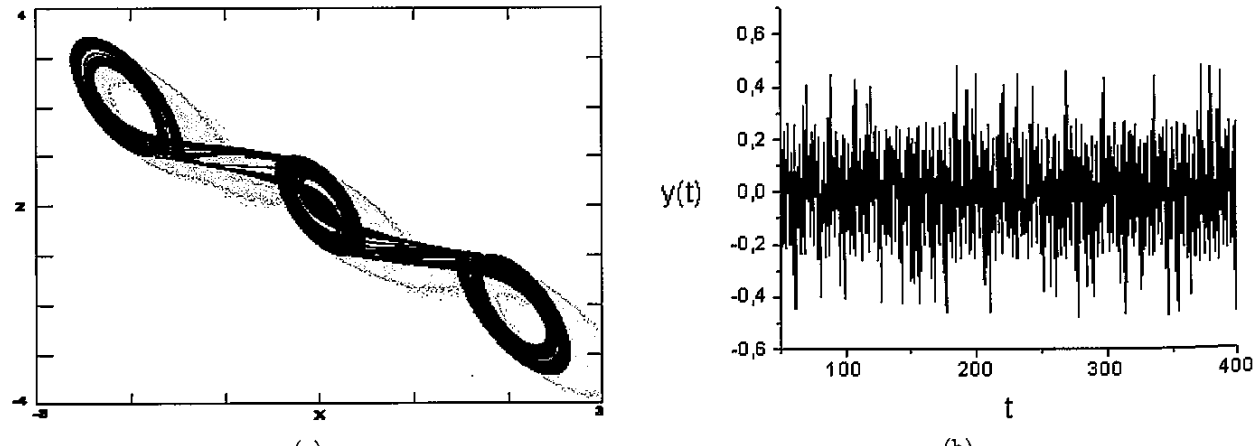

(a) (b)

Fig. 7. Projection onto the x–z plane of the 3-scroll chaotic attractor obtained for: $\alpha = 10.0, \beta = 14, a = 1$. (b) Time waveform of the time series $y(t)$.

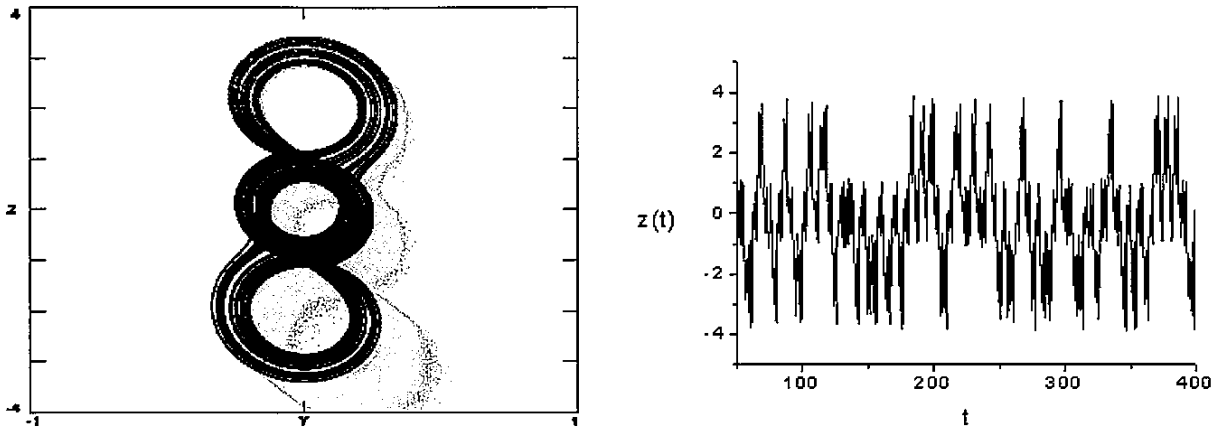

(a) (b)

Fig. 8. Projection onto the y–z plane of the 3-scroll chaotic attractor obtained for: $\alpha = 10.0, \beta = 14, a = 1$. (b) Time waveform of the time series $z(t)$.

Lyapunov exponent plots shown in Figs. 9(a) and 10(a) below and the bifurcation diagrams given in Figs. 9(b) and 10(b) seem to agree. The method essentially takes a numerical derivative and gives the correct result provided care is taken to ensure that the perturbed and unperturbed orbits lie on the same side of the discontinuity. This may require an occasional small perturbation into a region that is not strictly accessible to the orbit. Still a question arises about the exact value of the positive Lyapunov exponents.

In all these numerical methods, the data are calculated in double precision. Thus for $\alpha = 10.0$, $\beta = 14.0, m_0 = -0.43, m_1 = 0.41$, and $a = 1.0$, the system (3)–(4) has the 3-scroll chaotic attractor shown in Figs. 6(a), 7(a) and 8(a) with the waveforms of the time series $x(t), y(t), z(t)$ shown respectively in Figs. 6(b), 7(b) and 8(b).

The attractor shown in Figs. 6–8 resembles the so-called *three-scroll chaotic attractor*, but with only three equilibria, contrary in the usual case where this attractor requires at least five equilibria [Aziz-Alaoui, 1999].

Figures 9(a), 10(a), and 11(a) show the bifurcation diagrams of the variable y_n plotted versus control parameters $\alpha \in [0, 11.0]$, with $\beta = 14.0, \beta \in [0, 40.0]$, with $\alpha = 10.0$, and $a \in [0, 4.0]$, and with $\alpha = 10.0, \beta = 14.0$, respectively. In all these cases, the chaotic attractors are obtained via a border collision bifurcation scenario from a stable period-2 orbit. On the other hand, Figs. 9(b), 10(b) and 11(b) show the variations of the largest

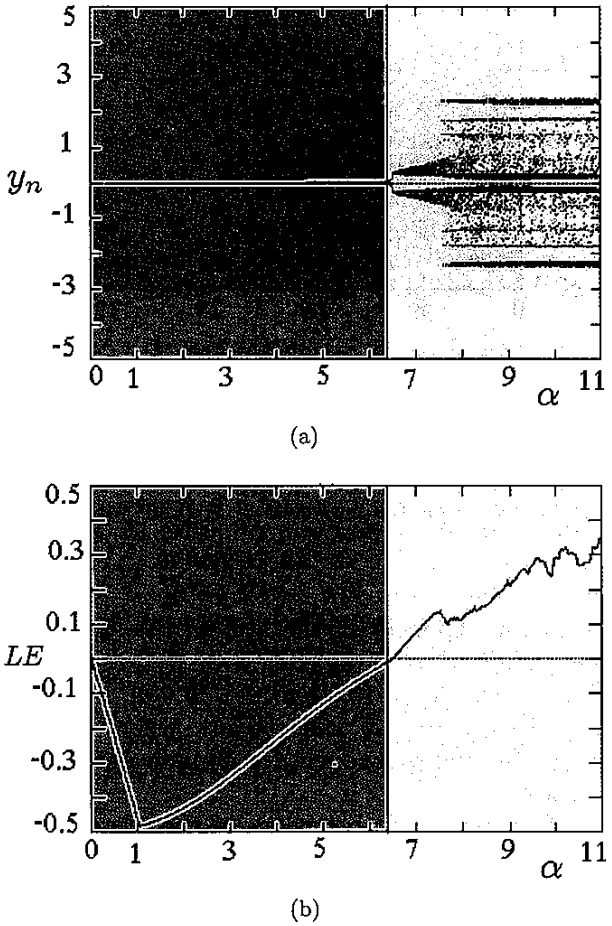

(a)

(b)

Fig. 9. (a) Bifurcation diagram of the variable y_n plotted versus control parameter $\alpha \in [0, 11]$ with $a = 1, \beta = 14$. (b) Variations of the largest Lyapunov exponent of the system (3)–(4) versus the parameter $\alpha \in [0, 11]$ with $a = 1$, $\beta = 14$.

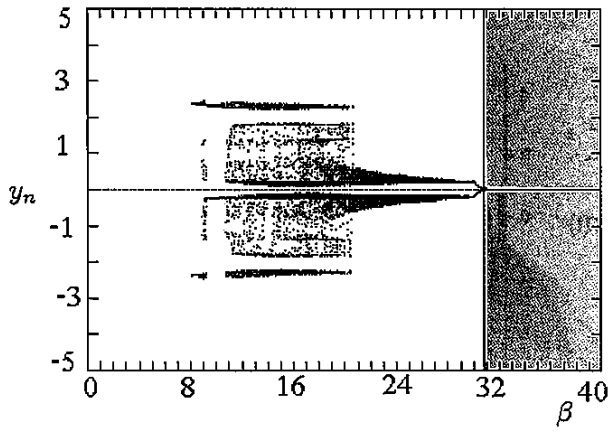

(a)

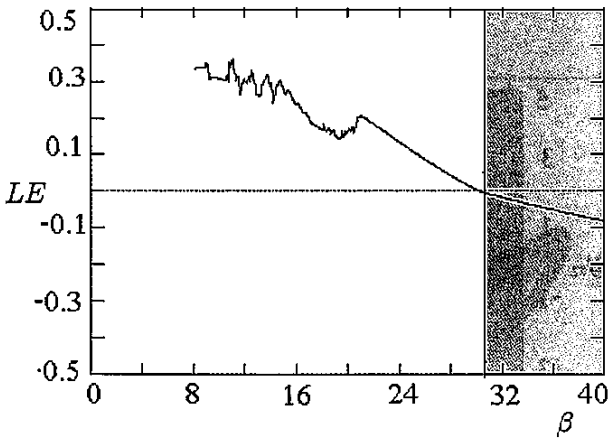

(b)

Fig. 10. (a) Bifurcation diagram of the variable y_n plotted versus control parameter $\beta \in [0, 40]$ with $a = 1, \alpha = 10$. (b) Variations of the largest Lyapunov exponent of the system (3)–(4) versus the parameter $\beta \in [0, 40]$ with $a = 1$, $\alpha = 10$.

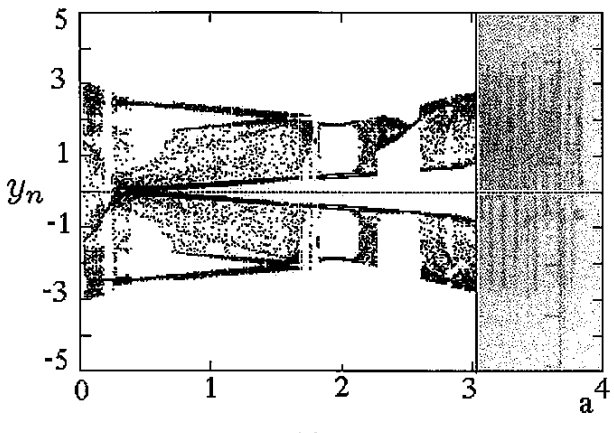

(a)

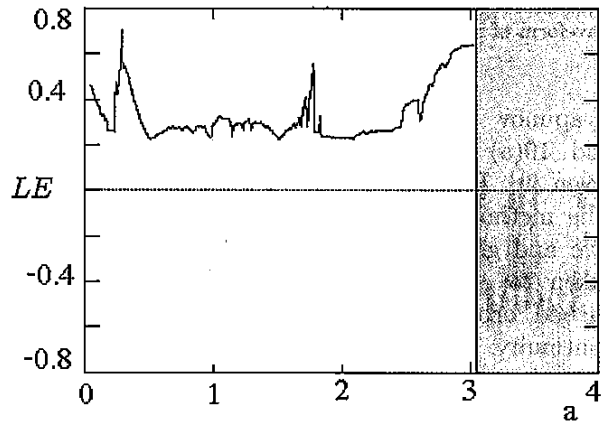

(b)

Fig. 11. (a) Bifurcation diagram of the variable y_n plotted versus control parameter $a \in [0, 4]$ with $\alpha = 10, \beta = 14$. (b) Variations of the largest Lyapunov exponent of the system (3)–(4) versus the parameter $a \in [0, 4]$ with $\alpha = 10$, $\beta = 14$.

Lyapunov exponent of the system (3)–(4) versus the parameter $\alpha \in [0, 11.0]$ with $\beta = 14.0, \beta \in [0, 40.0]$, with $\alpha = 10.0$ and $a \in [0, 4.0]$, and with $\alpha = 10.0, \beta = 14.0$, respectively, where positive largest Lyapunov exponent (LLE) indicates chaotic behavior.

The dynamical behaviors of the system (3)–(4) are investigated numerically. Fix parameters $\beta = 14.0, a = 1.0$, and let $\alpha > 0$ vary. The system (3)–(4) exhibits the following dynamical behaviors: When $0 \leq \alpha < 6.44$, the system converges to an equilibrium point. When $6.44 \leq \alpha < 6.5$, the system converges to a stable period-2 orbit. When $6.5 \leq \alpha < 7.62$, the system converges to a 1-scroll chaotic attractor as shown in Fig. 4(a) with the time waveform of $x(t)$ shown in Fig. 4(b). When $\alpha \geq 7.62$, the system converges to the 3-scroll chaotic attractor as shown in Figs. 6–8.

On the other hand, fix parameters $\alpha = 10.0$ and $a = 1.0$, and let $\beta > 0$ vary. The system (3)–(4) exhibits the following reverse (to the one with respect to α) dynamical behaviors: When $0 < \beta \leq 8.0$, the system converges to a periodic orbit. When $8.0 < \beta < 20.57$, the system converges to the 3-scroll chaotic attractor. When $20.57 \leq \beta < 29.97$, the system (3)–(4) converges to a 1-scroll chaotic attractor. When $29.97 \leq \beta < 31$, there is a limit cycle. When $\beta \geq 31.0$, the system converges to an equilibrium point. For $\alpha = 10.0, \beta = 14.0$, and $0 \leq a \leq 4.0$ varies, the system (3)–(4) is chaotic

and displays both the 1-scroll and 3-scroll chaotic attractors until a is in a small neighborhood of $a = 3.0$ where the system converges to a periodic orbit.

Note that all 3-scroll chaotic attractors appear when $a \leq 2.0488$ because the system (3)–(4) has three equilibria, but for $a > 2.0488$, the system (3)–(4) has at most one-scroll chaotic attractors because it has only one equilibrium point. On the other hand, one can observe that the so-called *double-scroll* can occur for some small values of a, for example for $0 < a < 0.17$ as shown in Fig. 5(a) with the time waveform of $x(t)$ shown in Fig. 5(b).

4. Conclusion

In this work we demonstrated numerically the existence of a 3-scroll chaotic attractor with three equilibria obtained from direct modification of Chua's equation. The new system (3)–(4) has some properties similar to the original Chua's system and other well-known modified Chua's systems. Some detailed analysis of the dynamics of this system was also presented.

References

Altman, E. J. [1993] "Bifurcation analysis of Chua's circuit with application for low-level visual sensing," *J. Circuit Syst. Comput.* **3**, 63–92.

Aziz-Alaoui, M. A. [1999] "Differential equations with multispiral attractors," *Int. J. Bifurcation and Chaos* **9**, 1009–1039.

Bilotta, E., Pantano, P. & Stranges, S. [2007] "A gallery of Chua attractors Part I," *Int. J. Bifurcation and Chaos* **17**, 1–60.

Brown, R. [1992] "Generalizations of the Chua equations," *Int. J. Bifurcation and Chaos* **2**, 889–909.

Chua, L. O., Komuro, M. & Matsumoto, T. [1986] "The double scroll family. Parts I and II," *IEEE Trans. Circuits Syst.* **33**, 1073–1118.

Chua, L. O. & Lin, G. N. [1990] "Canonical realization of Chua's circuit family," *IEEE Trans. Circuits Syst.* **37**, 885–902.

Hartley, T. T. & Mossayebi, F. [1993] "Control of Chua's circuit," *J. Circuit Syst. Comput.* **3**, 173–194.

Kal'yanov, E. [2003] "A two-circuit modification of the Chua chaotic oscillator," *Radiotekhnika i Elektronika* **48**, 339–344.

Karadzinov, L. V., Jefferies, D. J., Arsov, G. L. & Deane, J. H. B. [1996] "Simple piecewise-linear diode model for transient behavior," *Int. J. Electron.* **78**, 143–160.

Khibnik, A. J., Roose, D. & Chua, L. O. [1993] "On periodic orbit and homoclinic bifurcation in Chua's circuit with smooth non-linearity," *Int. J. Bifurcation and Chaos* **3**, 363–384.

Lamarque, C., Janin, O. & Awrejcewicz, J. [1999] "Chua systems with discontinuities," *Int. J. Bifurcation and Chaos* **9**, 591–616.

Lü, J., Zhou, T., Chen, G. & Yang, X. [2002] "Generating chaos with a switching piecewise-linear controller," *Chaos* **12**, 344–349.

Lü, J., Yu, X. & Chen, G. [2003] "Generating chaotic attractors with multiple merged basins of attraction: A switching piecewise-linear control approach," *IEEE Trans. Circuits Syst.-I, Fund. Th. Appl.* **50**, 198–207.

Lü, J., Han, F., Yu, X. & Chen, G. [2004a] "Generating 3-D multi-scroll chaotic attractors: A hysteresis series switching method," *Automatica* **40**, 1677–1687.

Lü, J., Chen, G., Yu, X. & Leung, H. [2004b] "Design and analysis of multiscroll chaotic attractors from saturated function series," *IEEE Trans. Circuits Syst.-I* **51**, 2476–2490.

Lü, J., Yu, S. M., Leung, H. & Chen, G. [2006] "Experimental verification of multi-directional multi-scroll chaotic attractors," *IEEE Trans. Circuits Syst.-I* **53**, 149–165.

Lü, J., Murali, K., Sinha, S., Leung, H. & Aziz-Alaoui, M. A. [2008] "Generating multi-scroll chaotic attractors by thresholding," *Phys. Lett. A* **372**, 3234–3239.

Mahla, A. I. & Badan Palhares, A. G. [1993] "Chua's circuit with discontinuous non-linearity," *J. Circuit Syst. Comput.* **3**, 231–237.

Parker, T. S. & Chua, L. O. [1989] *Practical Numerical Algorithms for Chaotic Systems* (Springer-Verlag, NY).

Sprott, J. C. [2000] "A new class of chaotic circuit," *Phys. Lett. A* **266**, 19–23.

Sprott, J. C. [2003] *Chaos and Time-Series Analysis* (Oxford University Press, Oxford).

Suykens, J. A. K. & Vandewalle, J. [1993] "Generation of n-double scrolls ($n = 1, 2, 3, 4, \ldots$)," *IEEE Trans. Circuits Syst.-I, Fund. Th. Appl.* **40**, 861–867.

Tang, K., Man, K., Zhong, G. & Chen, G. [2003] "Modified Chua's circuit with $x|x|$," *Contr. Th. Appl.* **20**, 223–227.

Yalcin, M. E., Suykens, J. A. K., Vandewalle, J. & Ozoguz, S. [2002] "Families of scroll grid attractors," *Int. J. Bifurcation and Chaos* **12**, 23–41.

Yu, S. M., Lu, J. H., Tang, W. K. S. & Chen, G. [2006] "A general multiscroll Lorenz system family and its DSP realization," *Chaos* **16**, 033126, 1–10.

Yu, S. M., Tang, W. K. S., Lü, J. & Chen, G. [2008] "Generation of $n \times m$-wing Lorenz-like attractors from

a modified Shimizu–Morioka model," *IEEE Trans. Circuits Syst.-II* **55**, 1168–1172.

Yu, S. M., Tang, W. K. S., Lü, J. & Chen, G. [2009] "Generating $2n$-wing attractors from Lorenz-like systems," *Int. J. Circuit Th. Appl.*, in press.

Zeraoulia, E. [2006] "A new switching piecewise-linear chaotic attractor with two equilibria of saddle-focus type," *Nonlin. Phen. Compl. Syst.* **9**, 399–402.

Zeraoulia, E. [2007] "A new 3-D piecewise linear system for chaos generation," *Radioengeneering* **16**, 40–43.